



# Improving plasticity and work-hardening capability of $\beta$ -type bulk metallic glass composites by destabilizing $\beta$ phases



Long Zhang, Zhengwang Zhu, Huameng Fu, Hong Li, Haifeng Zhang\*

Shenyang National Laboratory for Materials Science, Institute of Metal Research, Chinese Academy of Sciences, Shenyang 110016, China

## ARTICLE INFO

### Keywords:

Bulk metallic glass composite  
Work-hardening  
Structural stability  
Martensitic transformation

## ABSTRACT

Ti/Zr-based bulk metallic glass composites (BMGCs) containing an *in-situ* formed  $\beta$  phase ( $\beta$ -type BMGCs) normally show a poor work-hardening capability or even work-softening during plastic deformation. The limited work-hardening capability of the  $\beta$  phase by the entanglement of dislocations cannot totally compensate the shear softening of the glassy matrix. In this work, a strategy is proposed to destabilize the  $\beta$  phase, and the BMGC containing a metastable  $\beta$  phase (metastable  $\beta$ -type BMGC) shows improved plasticity and work-hardening capability due to the deformation-induced phase transformation from  $\beta$ -Ti to  $\alpha'$ -Ti. The underlying principle for destabilizing  $\beta$  phases in BMGCs by adjusting the overall compositions and the structural origins for the improved plasticity and work-hardening capability of metastable  $\beta$ -type BMGCs are discussed. These findings shed light on developing metastable  $\beta$ -type BMGCs with excellent mechanical properties.

## 1. Introduction

Bulk metallic glasses (BMGs), also known as amorphous alloys, possess a long-range disordered atomic arrangement [1]. BMGs exhibit excellent properties, such as high strength, large elastic limit, and excellent corrosion resistance [2,3]. However, the plastic deformation of BMGs is highly localized in narrow shear bands [4], and a temperature rise together with dilatation in the shear bands results in shear-softening [5]. Therefore, BMGs normally show work-softening in compression [4–6] and do not exhibit any notable macroscopic plasticity in tension [7], which severely restricts their applications as engineering materials [8]. In order to overcome this drawback, bulk metallic glass composites (BMGCs) containing an *in-situ* formed soft crystalline phase and a glassy matrix have been developed [9–14]. During deformation, the soft and ductile crystalline phase yields first, and a stress concentration occurs in the around glassy matrix, which causes the nucleation of multiple shear bands [12,15]. This results in a relatively large plastic strain of BMGCs. According to the different types of the *in-situ* formed crystalline phases, the widely-studied BMGCs can be classified into two groups [11]: CuZr/Ti-based BMGCs containing *in-situ* formed B2 CuZr/Ti [16–22], which can be named as B2-type BMGCs, and Zr/Ti-based BMGCs containing *in-situ* formed  $\beta$ -Zr/Ti [12,23–29], which can be named as  $\beta$ -type BMGCs.

The metastable B2 CuZr phase with a cubic primitive structure (group space:  $Pm\bar{3}m$ ) in B2-type BMGCs can transform into two martensites: B33 (Cm) and B19' ( $P2_1/m$ ) during deformation [17].

This leads to a good plasticity and work-hardening capability of B2-type BMGCs [17]. Unlike B2-type BMGCs,  $\beta$ -type BMGCs were generally developed by adding a considerable amount of  $\beta$ -stabilizers, such as Nb [12,30], V [31] or Ta [32], etc., to Ti/Zr-based glass-forming alloys to promote the precipitation of  $\beta$  phase during casting. Therefore, the  $\beta$ -Ti/Zr phase in  $\beta$ -type BMGCs usually contains a high amount of  $\beta$ -stabilizers, which causes a very stable body-centered cubic (bcc) structure of the  $\beta$  phase. The  $\beta$  phase yields first and plastically deforms via dislocation glide during loading [32]. Although the pile-up and entanglement of dislocations work-harden the  $\beta$  phase [33], however, this contribution is normally insufficient to compensate the softening of the glassy matrix. Consequently, almost all  $\beta$ -type BMGCs exhibit a very limited work-hardening capability during compression and a work-softening behavior during tension [11,33]. For examples, Hofmann et al. have processed Zr-based [29] and Ti-based [28] BMGCs by a semi-solid treatment, and all these  $\beta$ -type BMGCs show work-softening and necking during tensile tests.

Although two previously reported metastable  $\beta$ -type BMGCs ( $Ti_{48}Zr_{27}Ni_6Ta_5Be_{14}$  by Oh et al. [30] and  $Ti_{47.5}Zr_{33}Cu_{5.8}Ni_3Be_{12.5}$  by Mu et al. [34]) show martensitic phase transformation during deformation, these two BMGCs were developed occasionally, and no practical guidance for designing such metastable  $\beta$ -type BMGCs has been reported yet. As a fact, developing metastable  $\beta$ -type BMGCs which can show deformation-induced martensitic transformation is notoriously difficult. This requires an appropriate metastability of the *in-situ* formed  $\beta$  phase. If the  $\beta$  phase is too stable, no martensitic phase transformation would occur during deforma-

\* Corresponding author.

E-mail address: [h Zhang@imr.ac.cn](mailto:h Zhang@imr.ac.cn) (H. Zhang).

tion of BMGCs [29,33], and on the other hand, if the  $\beta$  phase is too unstable, it would decompose into equilibrium  $\alpha$ -Ti and intermetallic phases during the solidification of BMGCs [35]. In this article, the compositions of the studied alloys are  $(\text{Ti}_{0.518}\text{Zr}_{0.355}\text{Co}_{0.026}\text{Be}_{0.101})_{100-x}\text{Cu}_x$  ( $x=8$  or  $5$ ) in atomic percent, which are denoted as C8 ( $\text{Ti}_{47.7}\text{Zr}_{32.6}\text{Co}_{2.4}\text{Be}_{9.3}\text{Cu}_8$ ) and C5 ( $\text{Ti}_{49.2}\text{Zr}_{33.7}\text{Co}_{2.5}\text{Be}_{9.6}\text{Cu}_5$ ), respectively. C5 was designed by decreasing the Cu-amount of 8% in C8 to 5% and keeping the mutual ratios of other elements unchanged. C8 is a stable  $\beta$ -type BMGC, while C5 is a metastable  $\beta$ -type BMGC. Although the formation of various microstructures of the Ti-Zr-Cu-Co-Be BMGCs has been studied previously [25], the influence of structural stability of  $\beta$  phases on deformation mechanisms and mechanical properties is thoroughly investigated in this article. The metastable BMGC (C5) shows the improved plasticity and work-hardening capability as compared with the stable BMGC (C8), which is attributed to the deformation-induced martensitic transformation from  $\beta$ -Ti to  $\omega$ -Ti in the metastable BMGC (C5).

## 2. Experiments

Master ingots of  $\text{Ti}_{47.7}\text{Zr}_{32.6}\text{Co}_{2.4}\text{Be}_{9.3}\text{Cu}_8$  (C8) and  $\text{Ti}_{49.2}\text{Zr}_{33.7}\text{Co}_{2.5}\text{Be}_{9.6}\text{Cu}_5$  (C5) were prepared by arc melting high-purity Ti, Zr, Co, Be and Cu metals (purities are over 99.8 wt%) in a Ti-gettered high-purity argon atmosphere. The ingots were melted four times to ensure the chemical homogeneity. The as-cast rods with a diameter of 8 mm were prepared by arc re-melting the master ingots and copper mold suction casting in the high-purity argon atmosphere. The specimens were transversely cut from the as-cast rods of two BMGCs for the characterization by means of X-ray diffraction (XRD, Philips PW 1050, Cu-K $\alpha$ ), scanning electron microscopy (SEM, Zeiss Supra 55) combined with energy-dispersive X-ray spectroscopy (EDS, Oxford), and transmission electron microscopy (TEM, FEI Tecnai F30). The volume fractions and particle sizes of  $\beta$  phase were measured by using a computer software (Image J: <http://imagej.nih.gov>), and the compositions of  $\beta$  phase were measured by the SEM-attached EDS. For the TEM observations, slices with a diameter of 3 mm were cut from the rods and were mechanically ground to a thickness of 45  $\mu\text{m}$ . Then the slices were dimpled to reduce the central thickness to about 10  $\mu\text{m}$ , and ion-milled using a Gatan 691 device with liquid nitrogen cooling. Samples with a dimension of 3 mm $\times$ 3 mm $\times$ 6 mm were cut from the central part of the as-cast rods for compression tests in an Instron 5582 testing machine equipped with a laser extensometer. At least three samples of each alloy were tested. The fractured samples were also characterized by XRD, SEM and TEM.

## 3. Results

### 3.1. Microstructures of as-cast $(\text{Ti}_{0.518}\text{Zr}_{0.355}\text{Co}_{0.026}\text{Be}_{0.101})_{100-x}\text{Cu}_x$ alloys

The XRD patterns of as-cast C8 and C5 are shown in Fig. 1(a). Diffraction peaks from a bcc phase are superimposed on a broad hump from an amorphous phase. The bcc phase in the current alloys is  $\beta$ -Ti phase ( $\text{Im}\bar{3}m$ ), which is a chemical disordered solid solution. A tiny diffraction peak occurs at about  $2\theta=29^\circ$  in C5, which is identified as  $\{0001\}$  peak of  $\omega$ -Ti [36]. Athermal  $\omega$ -Ti has a hexagonal structure with a space group of  $P6/mmm$ , and it often forms through the collapse of  $\{222\}_\beta$  planes along the  $\langle 111 \rangle_\beta$  direction in metastable  $\beta$ -Ti alloys during cooling [36,37]. The SEM micrographs of as-cast C8 and C5 are shown in Fig. 1(b) and (c), respectively. The darker and isolated phase is  $\beta$ -Ti, and the brighter and continuous phase is amorphous matrix. Different with the previously reported dendrite-like morphology of  $\beta$  phase, the current  $\beta$ -Ti phase shows particle-like morphology, and the particles are well-ripened secondary arms of  $\beta$ -Ti dendrites [25]. With the decrease of Cu amount from 8% in C8 to 5% in C5, the particle sizes and the volume fractions of the  $\beta$  phase slightly increase from  $6 \pm 2 \mu\text{m}$  to  $7 \pm 2 \mu\text{m}$  and from  $59\% \pm 2\%$  to  $61\% \pm 2\%$ , respectively, as listed in

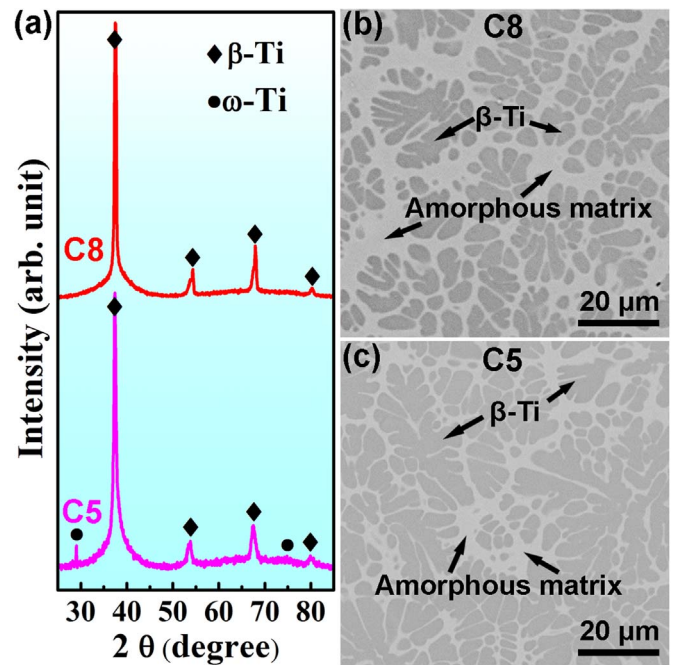


Fig. 1. XRD patterns (a) and the SEM back-scattered electron micrographs of as-cast 8 mm rods of C8 (b) and C5 (c) alloys. Both C8 and C5 alloys are  $\beta$ -type BMGCs.

Table 1. The compositions of the  $\beta$  phase were obtained by the SEM-attached EDS, and the results are also listed in Table 1. The contents of Ti, Zr and Co of  $\beta$  phases in two BMGCs do not show big differences, while the content of Cu decreases from  $3.8\% \pm 0.2\%$  in C8 to  $2.4\% \pm 0.2\%$  in C5. Although Be cannot be detected by EDS, previous work shows that almost all Be atoms dissolve in the glassy matrices of  $\beta$ -type BMGCs [12,29,38], and  $\beta$  phases can be treated as Be-free [12,29].

In order to reveal the microstructures in details, the specimens cut from the as-cast rods of C8 and C5 were characterized by TEM. Fig. 2(a) shows the typical microstructure of C8: the isolated  $\beta$  particles are embedded in the continuous glassy matrix. The selected area electron diffraction (SAED) pattern (inset in Fig. 2(a)) from the  $\beta$  phase under a zone axis of  $[110]_\beta$  clearly shows the diffraction spots from a single bcc crystal of  $\beta$ -Ti. The TEM micrograph of C5 (Fig. 2(b)) is similar to that of C8. The SAED pattern (upper inset in Fig. 2(b)) from the  $\beta$  phase in C5 was also obtained under a zone axis of  $[110]_\beta$ . Except the diffraction spots from the  $\beta$  phase, extra diffraction spots with weak intensities are visible and are located at positions of  $1/3\{112\}_\beta$  and  $2/3\{112\}_\beta$ . These spots are identified as  $\omega$  phase [37]. This suggests that a small fraction of  $\omega$  phase exists in  $\beta$  phase of C5, which is consistent with its XRD result. The amorphous nature of the continuous matrix was also confirmed by the diffuse ring in its SAED pattern (lower inset in Fig. 2(b)).

### 3.2. Room-temperature compressive stress-strain curves

The plots of true stress ( $\sigma$ ) versus logarithmic strain ( $\epsilon$ ) of C8 and C5 under compression are shown in Fig. 3(a). C8 yields at a true stress of  $1280 \pm 10$  MPa and a logarithmic strain of  $1.7 \pm 0.1\%$ . After yielding, the true stress of C8 increases slightly and continuously to the maximum stress of  $1535 \pm 10$  MPa at a logarithmic strain of  $7.1 \pm 0.1\%$ , and then the stress quickly decreases to a fracture stress of  $1520 \pm 20$  MPa at the fracture strain of  $7.4 \pm 0.2\%$ . C5 yields at a true stress of  $1110 \pm 10$  MPa and a logarithmic strain of  $1.7 \pm 0.1\%$ . After yielding, the true stress of C5 increases significantly to the maximum stress of  $1670 \pm 10$  MPa at a logarithmic strain of  $10.8 \pm 0.1\%$ , and then the true stress begins to decrease to a final fracture stress of  $1580 \pm 20$  MPa at the fracture strain of  $12.0 \pm 0.2\%$ , which is much larger than the fracture strain of  $7.4 \pm 0.2\%$  of C8.

The corresponding plots of work-hardening rate against logarithmic

Download English Version:

<https://daneshyari.com/en/article/5456524>

Download Persian Version:

<https://daneshyari.com/article/5456524>

[Daneshyari.com](https://daneshyari.com)